The Double-Wavelength Technique—An Alternative Technique to Determine Thermodynamic Temperature

E. R. Woolliams · R. Winkler · S. G. R. Salim · P. M. Harris · I. M. Smith

Abstract   Filter radiometry provides thermodynamic temperatures traceable to a cryogenic radiometer. An alternative technique is possible which provides absolute thermodynamic temperature through a different traceability chain, with the radiometric measurements purely relative. If this technique could be experimentally realized with similar uncertainties to those associated with filter radiometry, then this would provide a metrologically valuable 'second opinion' that would test for systematic effects common to all filter radiometry measurements. This paper describes the theoretical analysis prior to an experimental investigation of this technique. This theoretical analysis implies that with Re-C and Cu as the two blackbodies, the Re-C temperature can be determined with an uncertainty of approximately twice that expected with filter radiometry. For higher-temperature metal-carbide/carbon eutectics, the uncertainty difference would be smaller.

Keywords   Eutectic · Fixed points · Thermodynamic temperature

1 Introduction

Filter radiometry has developed such that the thermodynamic temperature of blackbody sources can now be determined routinely with high accuracy. At high temperatures, a new *mise en pratique* is likely to allow absolute radiometry for direct temperature measurement. For those without access to radiometric calibration facilities, this will be mediated by high-temperature fixed points, the temperature of which will be determined over the next few years as part of an international project organized by the Working Group 5 of the Consultative Committee for Thermometry of the

E. R. Woolliams (✉) · R. Winkler · S. G. R. Salim · P. M. Harris · I. M. Smith
National Physical Laboratory, Hampton Road, Teddington, Middlesex TW11 0LW, UK
e-mail: emma.woolliams@npl.co.uk

International Committee of Weights and Measures. The thermodynamic temperature of the cells will be determined by the world's best radiometric techniques—all of which will be variations of filter radiometry.

Filter radiometry is based on the measurement of total spectral flux from a black-body source within a narrow wavelength range [1, 2]. From this measurement, and Planck's law, the temperature of the blackbody source can be determined directly. In its simplest case, filter radiometry uses an instrument consisting of a spectrally filtered detector and two apertures. The spectral responsivity of the filtered detector is calibrated absolutely and traceably to a cryogenic radiometer [3] and the geometrical system, calibrated traceably to the meter, determines the proportion of flux seen. In many cases, there are advantages to add additional imaging optics—single or multiple lenses. Different national metrology institutes have different designs of primary filter radiometers and characterize these instruments in different ways. This is highly valuable to improve the community's understanding of systematic effects.

However, all filter radiometry-based systems have the same basic route of traceability. Filter radiometry provides thermodynamic temperature traceable via a cryogenic radiometer to the watt (optical power), via geometrical measurements of input apertures to the meter, and via a tuneable laser to the second (wavelength/frequency). An alternative technique is possible which provides absolute thermodynamic temperature through a different traceability chain, ultimately back to wavelength/frequency (only), with the radiometric measurements purely relative. If this technique could be experimentally realized with similar uncertainties to those associated with filter radiometry, then this would provide a metrologically valuable 'second opinion' that would test for systematic effects common to all filter radiometry measurements.

The double-wavelength technique was first proposed by Prokhorov et al. [4] but has not yet been proven experimentally. This paper describes how such an experiment could be realized.

2 Conceptual Design

If there are two blackbodies at temperatures T_1 and T_2, measured at two wavelengths λ_1 and λ_2, then the ratios of radiance of the blackbodies at each of these wavelengths are

$$
\begin{aligned}
x &= \frac{L_{\mathrm{BB}}(\lambda_1, T_1)}{L_{\mathrm{BB}}(\lambda_1, T_2)} = \frac{\left(\dfrac{c_{1L}/n^2}{\lambda_1^5(\exp[c_2/(n\lambda_1 T_1)]-1)}\right)}{\left(\dfrac{c_{1L}/n^2}{\lambda_1^5(\exp[c_2/(n\lambda_1 T_2)]-1)}\right)}, \\[2ex]
y &= \frac{L_{\mathrm{BB}}(\lambda_2, T_1)}{L_{\mathrm{BB}}(\lambda_2, T_2)} = \frac{\left(\dfrac{c_{1L}/n^2}{\lambda_2^5(\exp[c_2/(n\lambda_2 T_1)]-1)}\right)}{\left(\dfrac{c_{1L}/n^2}{\lambda_2^5(\exp[c_2/(n\lambda_2 T_2)]-1)}\right)},
\end{aligned}
\tag{1}
$$

can be measured, providing two equations and two unknowns (T_1 and T_2). The equations can be solved to obtain the two temperatures.

The radiometric measurements required are purely relative—the ratios of the radiances of the two blackbodies at each of two wavelengths. Note that this should not be confused with a two-color technique: the radiance at one wavelength is *not* compared to the radiance at another wavelength. The only absolute measurement is that to do with determining the wavelength.

3 Experimental Realization

The most likely experimental setup is shown in Fig. 1. A monochromator (with an order-sorting filter) would provide the wavelength selection, and off-axis parabolic mirrors would be used to focus light from each blackbody in turn into the monochromator. Alternative approaches, using, for example, narrow-band filters to provide wavelength selection and lenses to focus light from the blackbody, could be imagined—but may increase uncertainties.

3.1 Solution of Equation with Bandwidth

The most immediate problem with the experimental realization of this technique is that real measurements cannot be made at a single wavelength, but over a narrow range of wavelengths; thus, Eq. 1 becomes

$$
\begin{aligned}
x &= \frac{\int_{\lambda_1-\delta\lambda}^{\lambda_1+\delta\lambda} \frac{c_{1L}/n^2}{\ell^5(\exp[c_2/(n\ell T_1)]-1)} s_1(\lambda_1,\ell)\,\mathrm{d}\ell}{\int_{\lambda_1-\delta\lambda}^{\lambda_1+\delta\lambda} \frac{c_{1L}/n^2}{\ell^5(\exp[c_2/(n\ell T_2)]-1)} s_1(\lambda_1,\ell)\,\mathrm{d}\ell}, \\[2ex]
y &= \frac{\int_{\lambda_2-\delta\lambda}^{\lambda_2+\delta\lambda} \frac{c_{1L}/n^2}{\ell^5(\exp[c_2/(n\ell T_1)]-1)} s_2(\lambda_2,\ell)\,\mathrm{d}\ell}{\int_{\lambda_2-\delta\lambda}^{\lambda_2+\delta\lambda} \frac{c_{1L}/n^2}{\ell^5(\exp[c_2/(n\ell T_2)]-1)} s_2(\lambda_2,\ell)\,\mathrm{d}\ell},
\end{aligned}
\tag{2}
$$

where $s_1(\lambda_1,\ell)$ and $s_2(\lambda_2,\ell)$ are the bandpass functions for the monochromator at the short and long wavelengths, respectively. The influence of the finite bandwidth is
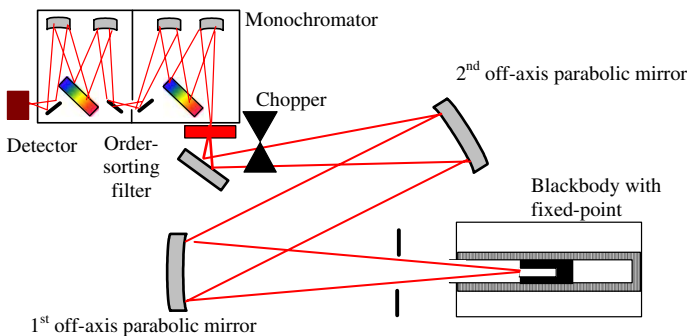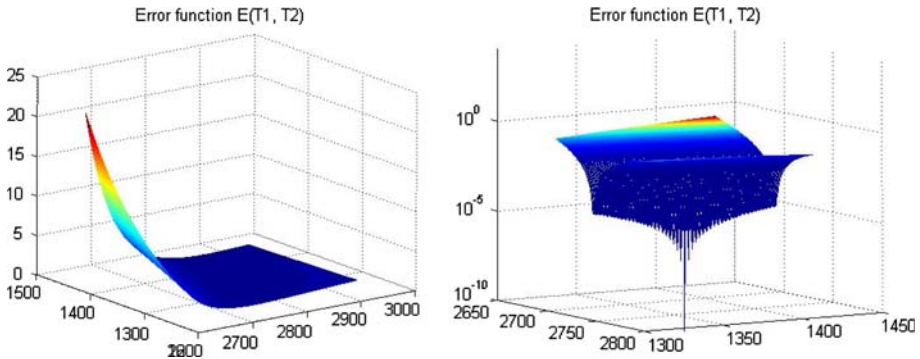

Fig. 1 Expected setup for measurements

Fig. 2 Error function to minimize (Eq. 3). This function in the left-hand plot appears to show a long 'valley' of potential solutions, and therefore no unique solution, although there is a single minimum with an error of zero (as seen by the logarithmic plot on the right)

too large to be ignored if accuracies approaching those of filter radiometry are to be achieved.

These two simultaneous equations can be solved using numerical techniques to obtain the temperature. The two ratios, x and y, can be calculated from estimates of the two temperatures and Eq. 2. These calculated ratios can be compared with the measured values and an error function minimized by standard numerical techniques. The error function to minimize is shown in Eq. 3. The normalization ensures that the x and y ratios are treated equally;

$$E = \frac{(x_{\mathrm{calc}} - x_{\mathrm{meas}})^2}{x_{\mathrm{meas}}^2} + \frac{(y_{\mathrm{calc}} - y_{\mathrm{meas}})^2}{y_{\mathrm{meas}}^2}. \tag{3}$$

We can visualize the function to be minimized by plotting E as a function of T_1 and T_2. From this, Fig. 2, for example, is obtained, in this case for Cu and Re-C at 700 nm and 4550 nm. The shape of the surface suggests that the problem might be numerically difficult to solve—the minimum of this function is not easy to determine and a range of values give very similar, and very small, values for the error function. However, when viewed on a logarithmic plot, it is clear that the 'required zero' indeed exists, and this can be found using high-level software functions, such as those provided by Matlab. The only problem is that the calculation can take several minutes, even on a powerful machine. This has implications for Monte Carlo uncertainty analysis, as described in section 'Monte Carlo calculation'.

The 'valley' nature of the error function is a by-product of the fact that the two temperatures are highly (positively) correlated—in the inevitable presence of measurement uncertainty, both temperatures will either be systematically over-estimated or under-estimated. See also section 'Implication of correlation'.

4 Experimental Design

Prior to any experimental work, it is important to determine whether the technique could realistically achieve uncertainties comparable with those of filter radiometry and to make decisions on, for example, which wavelengths should be used to determine the ratios. In order to make these decisions, the expected uncertainties associated with the two blackbody temperatures given different choices were determined using Monte Carlo simulation, described in more detail in section 'Monte Carlo calculation'. Because the Monte Carlo simulation took many hours for processing when bandwidth was considered, most of these preliminary tests were done using Eq. 1 rather than Eq. 2 to determine the calculated ratios in Eq. 3.

4.1 Choice of Blackbodies

Preliminary calculations showed that if the Cu-point is chosen as the lower-temperature blackbody, the uncertainty is similar for all the metal-carbon eutectics with temperatures higher than that of Pt-C. Since the uncertainty associated with filter radiometry increases with temperature, the double-wavelength technique will be most 'competitive' for higher-temperature eutectics. We have decided to start our investigations with Re-C and Cu as the two fixed points.

4.2 Choice of Wavelength

The uncertainty associated with the determined temperatures decreases as the two wavelengths become further apart, all else being equal. However, this decrease flattens off at long wavelengths (Fig. 3).
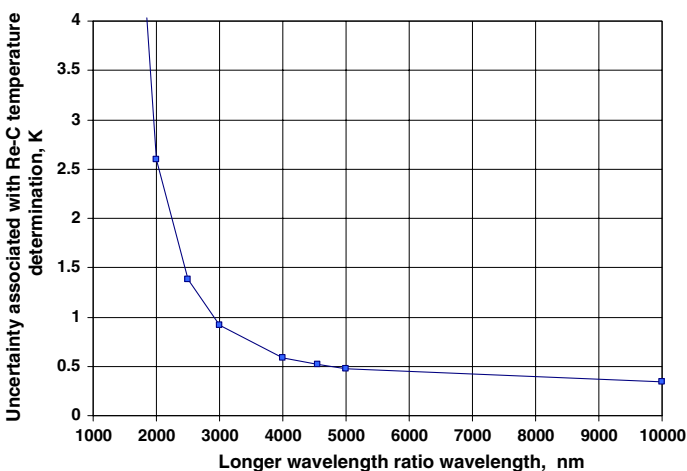
Fig. 3 Uncertainty associated with the Re-C blackbody temperature for different choices of the longer wavelength, given that the lower wavelength is 700 nm

If too short a wavelength is chosen, the large difference in signal level between the two blackbodies puts a stringent demand on measurement linearity, making it more difficult to determine the x-ratio with sufficient accuracy. However, the choice is reasonably arbitrary below 800 nm. We have chosen a wavelength of 700 nm so that we can use a tuneable Ti-sapphire laser to determine the bandpass function (see section 'Measuring the bandpass function').

For the longer wavelength, we need to avoid strong atmospheric absorption—for example, that due to water between 5 µm and 8 µm, or that between 4.15 µm and 4.4 µm due to carbon dioxide. However, between these regions there is a 'window' where atmospheric transmittance is high and the responsivity of InSb detectors is near its peak, so a wavelength around 4.55 µm is a good wavelength to choose. 10 µm is another potential wavelength, but it is significantly more difficult to work at, due to the performance of sources and detectors, with little real gain.

4.3 Measuring the Shorter Ratio

The shorter wavelength should be relatively straightforward to measure. At 700 nm, the Re-C blackbody is around 2,000 times brighter than a Cu blackbody. However, this is well within the linearity range of a silicon photodiode. A current-to-voltage converting amplifier will also be required, and the gain of this will need to be changed over three decades, but high-precision amplifiers have been designed for these applications and can be well characterized.

4.4 Measuring the Longer Ratio

The most appropriate detector for wavelengths around 4.55 µm is the InSb detector. However, this detector responds from below 1 µm to 5.5 µm, and therefore will be highly sensitive to stray light and emission from room-temperature sources. Therefore, we have chosen to narrow the spectral range using a filter radiometer, with a 200 nm bandpass filter cooled to 77 K, behind the monochromator. This provides a number of advantages, most notably improving the noise-equivalent power, which also allows the pre-amplifier gain to be increased by at least a factor of 10. The bandpass filter reduces the background incident on the detector; the wavelength selection, with a narrower bandwidth, will still be done with a monochromator.

The signal from the InSb detector will be pre-amplified and then extracted from the background using phase-sensitive detection techniques, through the use of a lock-in amplifier and a mechanical chopper in the optical beam [5]. However, this does place demands on the linearity of the lock-in amplifier. An alternative solution to this problem would be to add another fast amplifier with a gain of approximately 4.3 so that the lock-in will see the same signal level for both blackbodies.

At these wavelengths, there is significant output from room-temperature emission. The 'dark' blades of the chopper will be only 5,000 times dimmer than the Cu-point blackbody. This means that, without additional care, the real ratio measured will be

$$y = \frac{L(\lambda_2, T_1) + L(\lambda_2, 293 \text{ K})}{L(\lambda_2, T_2) + L(\lambda_2, 293 \text{ K})} \tag{4}$$

This offset will introduce an error to the measured ratio of $\sim 0.015\%$. The use of a cold blackbody (at 77 K) determines, indirectly, $L(\lambda_2, 77 \text{ K}) + L(\lambda_2, 293 \text{ K})$ and removes the problem [6]. Care must be taken to ensure that the chopper blades are at the same temperature for the measurement of all three blackbodies. This means that the blades must be protected from the 'heat' and 'cold' of the three blackbodies.

4.5 Measuring the Bandpass Function

The monochromator bandpass must be determined accurately. The most appropriate way to do this will be to spectrally tune a laser across the bandwidth of the monochromator. Rotating the monochromator grating will not be as accurate. The laser must illuminate the monochromator in exactly the same way as the blackbody does. Since the blackbody is a Lambertian source with a 3 mm aperture, to give the laser the same properties, an integrating sphere with a 3 mm aperture can be used.

It will be necessary to determine the bandpass of the monochromator over the full bandwidth and over a considerable region either side in order to determine any 'out-of-band' shape to the transmittance. With the short-wavelength ratio, this can be achieved using a Ti:sapphire laser.

Measuring the transmittance for the long wavelength requires tuneability over the range from, say, 4,300 nm to 4,800 nm. There are tuneable lasers in this wavelength range (lead salt diodes). The difficulty with using these sources is in knowing the exact wavelength. Wavemeters for this region based on PbSe detectors require far too strong a signal for this application, so a Fourier transform infrared radiometer (FTIR) system will be used instead. Higher orders of a tuneable visible/NIR laser could be used as part of a feasibility study, but would probably not be accurate enough for the main measurement as the output beam is less uniform for higher orders than for the first order.

5 Determining Uncertainties

5.1 Sources of Uncertainty

The sources of uncertainty that are considered are given in Table 1. The approximate values listed are rough estimates at this stage—they will need to be verified once the experiment has been performed.

A model for the measured ratios that includes these experimental effects is given by

$$
\begin{aligned}
x &= (1 + e_1) \left(\frac{\int L_{\text{BB}}(\ell, T_1 + e_{7,x}) \, s_1(\lambda_1 + e_5, \ell) \, d\ell + e_{3,\text{top}}}{\int L_{\text{BB}}(\ell, T_2 + e_{8,x}) \, s_1(\lambda_1 + e_5, \ell) \, d\ell + e_{3,\text{bottom}}} \right), \\
y &= (1 + e_2) \left(\frac{\int L_{\text{BB}}(\ell, T_1 + e_{7,y}) \, s_2(\lambda_2 + e_6, \ell) \, d\ell + e_{4,\text{top}}}{\int L_{\text{BB}}(\ell, T_2 + e_{8,y}) \, s_2(\lambda_2 + e_6, \ell) \, d\ell + e_{4,\text{bottom}}} \right),
\end{aligned} \tag{5}
$$

	Source of uncertainty	Approximate value
Table 1 Standard uncertainties associated with the double-wavelength technique		
1	Multiplicative error in the x-ratio, from, e.g., non-linearity	0.01 %
2	Multiplicative error in the y-ratio	0.005 %
3	Additive error in the x-ratio (top and bottom, uncorrelated),from, e.g., measurement noise	0.1 pA cf signal of 0.85 µA for Re-C and 0.4 nA for Cu
4	Additive error in the y-ratio (top and bottom, uncorrelated)	0.1 pA cf signal of 1.2 µA for Re-C and 0.3 µA for Cu
5	Systematic wavelength error in the x-ratio (wavelength offset common to both measurements)	0.01 nm
6	Systematic wavelength error in the y-ratio	0.05 nm
7	Re-C melting point temperature variation from the x-ratio measurement to the y-ratio	20 mK
8	Cu melting point temperature variation from the x-ratio measurement to the y-ratio measurement	5 mK
9	Noise in the determination of the bandpass function for the x-ratio	0.5 %
10	Noise in the determination of the bandpass function for the y-ratio	1 %
11	Uncorrelated wavelength offsets in individual measurements for the bandpass function determination, x-ratio	0.01 nm
12	Uncorrelated wavelength offsets in individual measurements for the bandpass function determination, y-ratio	0.02 nm

The estimated values for these uncertainty components may be subject to considerable correction once the technique is tested experimentally

where the effects e_i correspond to the different sources of uncertainty given in the table.

5.2 Monte Carlo Calculation

Because of the complexity of the model, the uncertainties associated with the estimated temperatures will be evaluated using a Monte Carlo method. This approach accounts fully for the non-linearity of the model and the probability distributions (Gaussian, rectangular, etc.) used to characterize all input quantities to the model that are subject to uncertainty. Each uncertainty component listed in Table 1 is characterized by a Gaussian distribution and has the effect on the overall calculation as described in Eq. 5, which in turn feeds into the function to be minimized (Eq. 3). If all effects are included, this provides an overall assessment of the uncertainty associated with the estimated temperatures. If individual effects are included, this provides valuable information about which effects are dominant and therefore where the experimental effort should be focussed.
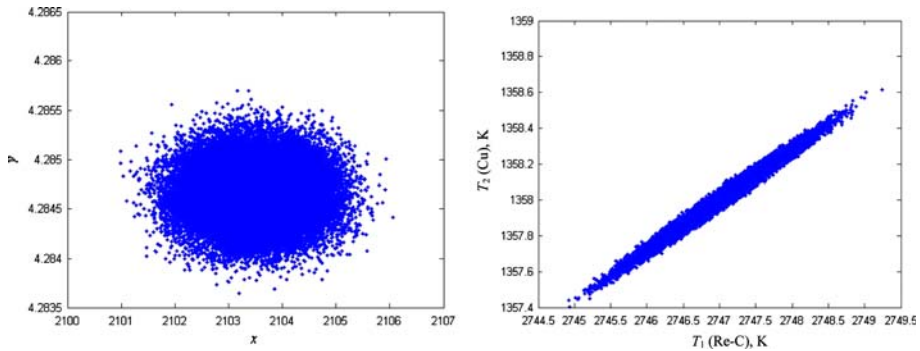
Fig. 4 Left: input x and y values for the two ratios as determined by the random-number generation and the uncertainty model; right: thermodynamic temperatures of Re-C (T_1) and Cu (T_2) as calculated using Monte Carlo method

The problem with the Monte Carlo calculation is that each trial takes several minutes of computational time once the bandwidth is fully considered. Thus, to provide statistically valid results, which requires many thousands of trials, the calculations can take days. To get around this, software was written to use the power of the NPL-grid—allowing calculations to be performed simultaneously on some 100 computers. A paper [7] and dissertation [8] describe the mathematics and software developments required to ensure that this approach is valid, for example, that the different computers did not generate the same random numbers.

6 Results of Experimental Modeling

6.1 Achievable Uncertainties

If the uncertainties listed in Table 1 are used and the measurement wavelengths are 700 nm, with a 3 nm bandpass measured at nine intermediate wavelengths, and 4,550 nm, with an 85 nm bandpass also measured at nine intermediate wavelengths, then the overall standard uncertainty associated with the temperature of the Re-C point is 0.51 K and that associated with the temperature of the Cu point is 0.15 K. The input and results of the Monte Carlo calculations are given in Fig. 4.

The size of each source of uncertainty due to errors in both x- and y-ratios in each blackbody temperature is shown in Table 2.

One interesting result from this is the way in which the natural repeatability of the Re-C and Cu-point blackbodies has a much larger effect than its size would imply. This is an effect of the correlation between the two temperatures.

6.2 Implication of Correlation

It is immediately obvious from Fig. 4 that the two temperatures are highly correlated. In this example, the correlation coefficient is 0.99. This does not prevent the two

Table 2 Standard uncertainty associated with each blackbody temperature due to each source of uncertainty in Table 1

Source of uncertainty	Corresponding sources of uncertainty in Table 1	Uncertainty value at Re-C point (K)	Uncertainty value at Cu point (K)
Multiplicative errors in the x-ratio and the y-ratio	1, 2	0.35	0.09
Additive errors in the x-ratio and the y-ratio	3, 4	0.29	0.09
Systematic wavelength errors in the x-ratio and the y-ratio	5, 6	0.14	0.04
Re-C and Cu points temperature variations from the x-ratio measurement to the y-ratio	7, 8	0.14	0.04
Noise in the determination of the bandpass function for the x-ratio and the y-ratio	9, 10	0.13	0.03
Uncorrelated wavelength offsets in individual measurements for the bandpass function determination in x-ratio and the y-ratio	11, 12	0.04	0.01
All sources combined	1–12	0.51	0.15

temperatures from being determined—if sufficient independent realizations are made, then the average temperatures will be correct. However, this correlation also means that the uncertainty associated with the *difference* between the two blackbody temperatures will be smaller than the uncertainty associated with the estimate of each temperature. The uncertainty associated with the difference is given by

$$u^2 (T_2 - T_1) = u^2 (T_1) + u^2 (T_2) - 2\rho u (T_1) u (T_2). \qquad (6)$$

With an uncertainty associated with Re-C of 0.51 K, an uncertainty associated with Cu of 0.15 K, and a correlation coefficient of 0.99, the uncertainty associated with the difference is 0.37 K. If there were an entirely independent realization of Cu (for example, through filter radiometry) with an associated uncertainty of, say, 0.06 K, then it would be possible to use this method to determine the Re-C transition with

an associated uncertainty of 0.38 K (compared to a filter radiometric measurement of Re-C with an associated uncertainty of 0.25 K). For higher-temperature eutectics, the double-wavelength technique is likely to be more competitive. It is interesting to consider whether this information could be used to determine a more self-consistent set of temperatures when providing definitive values for the phase transitions of the different metal-carbon eutectics.

6.3 Possible Extensions

This method determines the temperature of two blackbodies based on ratio measurements at two wavelengths. By introducing additional wavelengths, the technique would have built in redundancy. This approach may provide additional information and is the basis of the concept of using FTIR spectrometers to determine an absolute temperature [9].

7 Summary

So far, there has not been an opportunity to carry out these experiments in the laboratory. However, the approach has clear potential. The measurement uncertainties expected from this technique are approximately twice those expected from filter radiometry at the Re-C melting-point temperature. This is sufficiently accurate to supply a metrologically useful second opinion. As the uncertainties are expected to be lower if the temperatures are further apart, the method would be even more valuable with TiC-C and ZrC-C blackbodies.

References

1. J. Fischer, H.J. Jung, Metrologia **26**, 245 (1989)
2. N.P. Fox, J.E. Martin, D.H. Nettleton, Metrologia **28**, 357 (1991)
3. N.P. Fox, Metrologia **32**, 535 (1995/96)
4. A.V. Prokhorov, S.N. Mekhontsev, V.I. Sapritsky, in *Proceedings of TEMPMEKO '99, 7th International Symposium on Temperature and Thermal Measurements in Industry and Science*, ed. by J. F. Dubbeldam, M.J. de Groot (Edauw Johannissen BV, Delft, 1999), pp. 698–703
5. E. Theocharous, Appl. Opt. **47**, 1090 (2008)
6. E. Theocharous, N.P. Fox, V.I. Sapritsky, S.N. Mekhontsev, S.P. Morozova, Metrologia **35**, 549 (1998)
7. T.J. Esward, A.D. Ginestous, P.M. Harris, I.D. Hill, S.G.R. Salim, I.M. Smith, B.A. Wichmann, R. Winkler, E.R. Woolliams, Metrologia **44**, 319 (2007)
8. A.D. Ginestous, Monte Carlo Methods for Uncertainty Analysis in Metrology and Their Application in a Parallel Processing Environment. Ph. D. Thesis, Heriot Watt University, 2006
9. A.G. Steele, N.L. Rowell, in *Proceedings of TEMPMEKO 2001, 8th International Symposium on Temperature and Thermal Measurements in Industry and Science*, ed. by B. Fellmuth, J. Seidel, G. Scholz (VDE Verlag, Berlin, 2002), pp. 383–388